A RIEMANNIAN DISTANCE APPROACH TO MIMO RADAR SIGNAL DESIGN

Y. Y. Shi[*], *J. Xu*[†], *K. M. Wong*[*†‡] Life Fellow, IEEE, *T. N. Davidson*[†] Fellow, IEEE

[*]School of Information Engineering, Zhengzhou University, China
[†]Department of Electrical and Computer Engineering, McMaster University, Canada

ABSTRACT

We consider the signal design problem for a Multi-Input Multi-Output (MIMO) radar. The goal is to design a signal vector having a desired covariance (CoV) matrix while ensuring that the sidelobes of the ambiguity functions are small. Since CoV matrices are structurally constrained, they form a manifold in the signal space. Hence, we argue that the difference between these matrices should not be measured in terms of the conventional Euclidean distance (ED), rather, the distance should be measured along the surface of the manifold, i.e., in terms of a Riemannian distance (RD). In either case, the signal optimization problem is quartic in the design variables. An efficient algorithm based on successive convex quadratic optimization is developed and is effective in producing good approximate solutions. Comparing the designs using ED and RD, we find that the convergence of the algorithm can be significantly faster by optimizing over the manifold (RD) than by optimizing in ED. More importantly, for tight constraints, the use of RD yields solutions which satisfy the constraints far better than the use of ED.

Index Terms— MIMO radar, signal design, Riemannian distance, convex optimization

1. INTRODUCTION

The MIMO radar, as a new type of radar system, was formally proposed in the beginning of the 21st century. Due to its various advantages [1] over the traditional single input single output (SISO) radar, the MIMO radar has aroused great interests among researchers around the world. Considerable effort has been dedicated to the design of the transmission signal and the synthesis of the waveform: Different methods [2, 3] aiming at matching given transmission beam patterns as well as minimizing the cross-correlation of reflected signals have been proposed. In particular, an algorithm to design a unimodulus signal set matching beam pattern specifications and suppressing sidelobes of both cross- and auto-correlations has been developed [4]. Instead of the beam pattern matching design, algorithms were presented in [5] and [6] to synthesize a waveform directly such that its covariance (CoV) matrix is close to a desired matrix $\mathbf{R}$, having good cross- and auto-correlation properties. Using various forms of weighting, the design problem was formulated as different mathematical expressions optimized under a low peak-to-average power ratio (PAR) constraint. Several computationally efficient Cyclic Algorithms (CA) were presented to design unimodular MIMO waveforms minimizing the distance between the CoV matrix and the desired matrix.

[‡]Corresponding author. Financial supports from Zhengzhou University and from NSERC, Canada is gratefully acknowledged.

In the methods mentioned above, the design objectives focus on the difference between the desired and the actual CoV matrices, and are all measured in terms of the commonly used *Euclidean distance* (ED), which is also often called [7] the *Frobenius distance* (FD). Being positive semi-definite and Hermitian symmetric, CoV matrices are structurally constrained and thus form a *manifold* $\mathcal{M}$ in the linear vector space $\mathcal{H}$ of all $M \times M$ matrices [8]. Therefore, the commonly used ED may not be appropriate for measuring the distance between two CoV matrices; rather, we should measure the distance along the surface of the manifold. Thus in this paper, we formulate the problem of designing the radar transmission signal having a CoV matrix close to a desired matrix, the distance between the two matrices being measured in terms of a metric suitable for measuring on a manifold, i.e., a *Riemannian distance* (RD).

In addition, we also aim at sharpening the main lobe and at suppressing the sidelobes of the MIMO ambiguity function [9, 10, 12, 13] so that the accuracy of estimating the delay and Doppler shift will be enhanced. For such a purpose, we develop a successive convex approximation algorithm (e.g., [14, 15]), in which we approximate the original non-convex quartic problem by a convex quadratic problem at each stage. The optimization using RD as the measure shows much faster convergence compared to the corresponding problem measured in ED. The use of RD also yields signal designs having higher accuracy in estimating the distances and velocities of the targets. Under tighter constraints, we also find cases in which the optimization using ED does not converge properly, whereas that using RD does.

2. SIGNAL MODEL AND AMBIGUITY FUNCTION

We consider a MIMO radar system equipped with M transmission antennas and M reception antennas. The signal to be transmitted from m^{th} antenna $x_m(t)$ is a linear combination of $K \geq M$ orthonormal unit-energy functions $s_k(t)$ such that

$$x_m(t) = \sum_{k=1}^{K} \alpha_{mk} s_k(t) = \boldsymbol{\alpha}_m^T \cdot \mathbf{s}(t) \tag{1}$$

where $\mathbf{s}(t) = [s_1(t) \ \ldots \ s_K(t)]^T$, $\boldsymbol{\alpha}_m = [\alpha_{m1} \ldots \alpha_{mK}]^T$. Let $\mathbf{x}(t) = [x_1(t) \ \ldots \ x_M(t)]^T$ denote the transmission signal vector, and let $\mathbf{A} = [\boldsymbol{\alpha}_1 \ \ \boldsymbol{\alpha}_2 \ \ldots \ \boldsymbol{\alpha}_M]^T$. Then, by discretizing each of the continuous-time vectors $\mathbf{s}(t)$ and $\mathbf{x}(t)$ to N samples, we can write

$$\mathbf{X} = \mathbf{AS}, \qquad \mathbf{X}, \mathbf{S} \in \mathbb{C}^{M \times N} \tag{2}$$

In a MIMO radar, the *cross-ambiguity function* (CAF) [1, 10] between two (pair-wise) signals $x_{m_1}(t)$ and $x_{m_2}(t)$ defined in Eq. (1) is given by:

$$\begin{aligned} f_{m_1 m_2}(\tau,\nu) &= \int x_{m_1}(t) x^*_{m_2}(t+\tau) e^{j2\pi\nu t} dt \\ &= \sum_{i=1}^{K}\sum_{j=1}^{K} \alpha_{m_1 i}\alpha^*_{m_2 j} \int s_i(t) s^*_j(t+\tau) e^{j2\pi\nu t} dt \\ &= \sum_{i=1}^{K}\sum_{j=1}^{K} \alpha_{m_1 i}\alpha^*_{m_2 j} \phi_{ij}(\tau,\nu) \end{aligned} \tag{3}$$

where $m_1, m_2 = 1, \cdots, M$, τ and ν denote time and Doppler frequency shifts, and $\phi_{ij}(\tau,\nu)$ denotes the CAF for $s_i(t)$ and $s_j(t)$. If $x_{m_1}(t)$ and $x_{m_2}(t)$ represent respectively the transmitted and returned radar signals, then the peak of $f_{m_1 m_2}(\tau,\nu)$ indicates the location of the time-delay and Doppler shift of the returned signal and thus the distance and velocity of the target can be estimated [11]. With $f_{m_1 m_2}(\tau,\nu)$ of Eq.(3) being the $m_1 m_2{}^{\text{th}}$ element, we can form the $M \times M$ *ambiguity matrix* for all the M transmitted signals of the MIMO radar,

$$\mathbf{F}(\tau,\nu) = \mathbf{A}\mathbf{\Phi}^T(\tau,\nu)\mathbf{A}^H \tag{4}$$

where $\mathbf{\Phi}(\tau,\nu)$ is a $K \times K$ matrix whose $(ij)^{\text{th}}$ element is $\phi_{ij}(\tau,\nu)$. We note that, since signals in $\{\mathbf{s}(t)\}$ are orthonormal, $\mathbf{\Phi}(0,0) = \mathbf{I}$, giving $\mathbf{F}(0,0) = \mathbf{A}\mathbf{A}^H$.

For a target at a direction θ to the normal of the transmission antenna array, the *MIMO radar AF* is given by [1, 10]

$$f(\tau,\nu,\theta) \;=\; \mathbf{a}_{\text{T}}^T(\theta)\cdot\mathbf{F}(\tau,\nu)\cdot\mathbf{a}_{\text{T}}^*(\theta) \tag{5}$$

where $\mathbf{a}_{\text{T}}(\theta)$ is the transmission array directional vector. The MIMO radar may use this function to estimate τ and ν. Thus, it is desirable to design, for the transmitted signals, an ambiguity matrix $\mathbf{F}(\tau,\nu)$ whose properties are advantageous to the estimation of τ and ν:

(i) For good correlation property, we need ideally
$f_{m_1 m_2}(0,0) = \begin{cases} 1 & m_1 = m_2 \\ 0 & m_1 \neq m_2 \end{cases} \Rightarrow \mathbf{F}_{\text{ideal}}(0,0) \to \mathbf{I}$
But from above, $\mathbf{F}(0,0) = \mathbf{A}\mathbf{A}^H$. Thus, the distance $d(\mathbf{A}\mathbf{A}^H, \mathbf{I})$ between $\mathbf{A}\mathbf{A}^H$ and $\mathbf{I}$ should be minimized.

(ii) For $m_1 = m_2$, $f_{m_1 m_2}(\tau,\nu)$ should decrease in magnitude from the $(0,0)$ point as fast as possible so that the time-delay and Doppler shift can be located sharply.

(iii) For all other values of $\tau, \nu \neq 0$, $|f_{m_1 m_2}(\tau,\nu)|$ should be small to avoid interfering with the main lobe.

3. OPTIMUM SIGNAL DESIGN

We now formulate the optimum signal design problem: We need to design M transmission signals $\{x_m(t)\}$ each synthesized with a set of orthonormal functions $\{s_k(t)\}$. The ambiguity matrix of the transmission signals should satisfy the three required properties mentioned above.

Euclidean and Riemannian Distances:
Property (i) requires us to minimize the distance, or equivalently, the squared distance $d^2(\mathbf{A}\mathbf{A}^H, \mathbf{I})$, between $\mathbf{A}\mathbf{A}^H$ and $\mathbf{I}$, both of which are positive definite and Hermitian (PDH) matrices. We can treat the two matrices as free elements in the signal space and employ the commonly used ED such that for two $M \times M$ matrices $\mathbf{P}_1$ and $\mathbf{P}_2$,

$$d^2_{\text{E}}(\mathbf{P}_1,\mathbf{P}_2) = \|\mathbf{P}_1 - \mathbf{P}_2\|_2^2 = \text{tr}(\mathbf{P}_1 - \mathbf{P}_2)(\mathbf{P}_1 - \mathbf{P}_2)^H \tag{6}$$

On the other hand, PDH matrices are structurally constrained and form a manifold in the signal space. An appropriate way of measuring the distance between two such matrices $\mathbf{P}_1$ and $\mathbf{P}_2$ is the RD which measures along the surface of the manifold. Three closed forms of RD, $d_{\text{R}_1}, d_{\text{R}_2}, d_{\text{R}_3}$, for such distance measure were derived [8]. In particular, d_{R_2}, which is more easily manipulatable mathematically, is given by:

$$d^2_{\text{R}_2}(\mathbf{P}_1,\mathbf{P}_2) = \|\mathbf{P}_1^{\frac{1}{2}} - \mathbf{P}_2^{\frac{1}{2}}\|_2^2 = \text{tr}\left[\mathbf{P}_1 + \mathbf{P}_2 - 2\mathbf{P}_1^{\frac{1}{2}}\mathbf{P}_2^{\frac{1}{2}}\right] \tag{7}$$

We will use both Eqs. (6) and (7) in our design and examine the effects on the performance of the MIMO radar.

For Property (ii), we can specify a "mask" at the neighbouring points of $(0,0)$ to limit the height, and thus the width, of the main lobe. Hence, if we specify $|f_{mm}(0,0)| = P_0\ \forall m$, we can control the main-lobe width by imposing element-wise constraints of the term $|f_{mm}(\pm\Delta\tau, \pm\Delta\nu)| \leq \beta P_0$ where $0 < \beta < 1$, $\Delta\tau$ and $\Delta\nu$ are small steps away from $(0,0)$ in the τ and ν directions respectively. The closer are these neighbouring points to (0,0), the narrower will be the main lobe.

For Property (iii), likewise, we can control the sidelobes by the constraints $|f_{m_1 m_2}(\tau,\nu)| \leq \epsilon(\tau,\nu)$ for suitably sampled value for τ and ν. To significantly reduce computation at the price of coarser control over the sidelobe, we can alternatively impose the norm constraints $\|\mathbf{F}(\tau,\nu)\|_2^2 \leq \epsilon(\tau,\nu)$.

Thus, our signal design problem can be formulated as:

$$\begin{aligned} &\text{(i)} \ \min_{\mathbf{A}} \ d^2\left(\mathbf{A}\mathbf{A}^H, \mathbf{I}\right) \\ \text{s.t.} \ &\text{(ii)} \ |f_{mm}(\pm\Delta\tau, \pm\Delta\nu)| \leq \beta P_0, \qquad m = 1, \cdots, M \\ &\text{(iii)} \ \|\mathbf{A}\mathbf{\Phi}^T(\tau_{\ell_1}, \nu_{\ell_2})\mathbf{A}^H\|_2^2 \leq \epsilon(\tau_{\ell_1}, \nu_{\ell_2}), \\ &\qquad \text{sample points } \tau_{\ell_1}, \nu_{\ell_2} \neq 0; \ \ \ell_1, \ell_2 = 1, \ldots, L \\ &\text{(iv)} \ [\mathbf{A}\mathbf{A}^H]_{mm} = 1 \end{aligned} \tag{8}$$

where the objective function $d(\cdot,\cdot)$ takes on either d_{E} in Eq. (6) or d_{R_2} in Eq. (7), and the last constraint stipulates the value of $f_{mm}(0,0)$, i.e., $P_0 = 1$ as well as the transmission power.

3.1. Approximating the Objective Function

- Using Eq. (6), the objective function becomes $d^2_{\text{E}}\left(\mathbf{A}\mathbf{A}^H, \mathbf{I}\right) = \|\mathbf{A}\mathbf{A}^H - \mathbf{I}\|_2^2$ which involves a quartic term.
- Using Eq. (7), the objective function becomes $d^2_{\text{R}_2}\left(\mathbf{A}\mathbf{A}^H, \mathbf{I}\right) = \|\left(\mathbf{A}\mathbf{A}^H\right)^{1/2} - \mathbf{I}^{1/2}\|_2^2$ which involves square root terms.

In either case, the objective function is not convex. We employ the successive convex approximation approach in the following way:

1. At the n^{th} iteration, we approximate $\mathbf{A}^{(n)}\mathbf{A}^{(n)H}$ by $\tilde{\mathbf{A}}^{(n)}\mathbf{A}^{(n-1)H}$.
   a) ED objective becomes:
   $$\hat{d}^2_{\text{E}}(\tilde{\mathbf{A}}^{(n)}\mathbf{A}^{(n-1)^H}, \mathbf{I}) = \left\| \tilde{\mathbf{A}}^{(n)}\mathbf{A}^{(n-1)^H} - \mathbf{I} \right\|_2^2 \quad (9)$$
   b) Applying the SVD to $\mathbf{A}^{(n-1)}$,
   $$\mathbf{A} = \mathbf{V}\mathbf{\Sigma}\mathbf{U}^H = \mathbf{V}[\underset{M\times M}{\tilde{\mathbf{\Sigma}}}\ \mathbf{0}] \begin{bmatrix} \tilde{\mathbf{U}}^H \\ \hline \tilde{\mathbf{U}}_0^H \end{bmatrix} = \mathbf{V}\tilde{\mathbf{\Sigma}}\tilde{\mathbf{U}}^H \quad (10)$$
   giving
   $$\mathbf{A}\tilde{\mathbf{U}} = \mathbf{V}\tilde{\mathbf{\Sigma}} \quad (11)$$
   Thus, from Eq. (10), we have
   $$\mathbf{A}\mathbf{A}^H = \mathbf{V}\tilde{\mathbf{\Sigma}}\tilde{\mathbf{\Sigma}}^H\mathbf{V}^H \qquad \text{yielding,}$$
   $$(\mathbf{A}\mathbf{A}^H)^{1/2} = \mathbf{V}\tilde{\mathbf{\Sigma}}\mathbf{V}^H = \mathbf{A}\tilde{\mathbf{U}}\mathbf{V}^H \quad (12)$$
   where the last step of Eq. (12) is from Eq. (11). Thus, the RD objective becomes:
   $$\hat{d}^2_{\text{R}_2}(\tilde{\mathbf{A}}^{(n)}\mathbf{A}^{(n-1)^H}, \mathbf{I}) = \|\tilde{\mathbf{A}}^{(n)}\tilde{\mathbf{U}}^{(n-1)}\mathbf{V}^{(n-1)^H} - \mathbf{I}\|_2^2 \quad (13)$$
   Both modified objectives Eqs. (9) and (13) are quadratic and are convex in $\tilde{\mathbf{A}}^{(n)}$. (Applying the same approximation, the constraints also become quadratic.)
2. Solve the resulting convex problem for an approximate solution $\tilde{\mathbf{A}}^{(n)}$.
3. Obtain $\mathbf{A}^{(n)}$ by $\mathbf{A}^{(n)} = \tilde{\mathbf{A}}^{(n)} + \gamma^{(n)}\left(\mathbf{A}^{(n-1)} - \tilde{\mathbf{A}}^{(n)}\right)$. ($\gamma^{(n)}$ being the step size.)

We summarize the optimum signal design algorithm for both ED and RD objective functions in Table 1.

Table 1. Successive Optimization Algorithm

Step 0	Select an initial matrix $\mathbf{A}^{(0)}$ with elements α_{mk}. Set $\gamma^0 = 1, n = 0$, and select a value for a.
Step 1	Update iteration index $n \longleftarrow n+1$
Step 2	(i) For ED, go to Step 3. (ii) For RD, perform an SVD of $\mathbf{A}^{(n-1)}$ to obtain $\tilde{\mathbf{U}}^{(n-1)}$ and $\mathbf{V}^{(n-1)}$
Step 3	Given $\mathbf{A}^{(n-1)}$, $\tilde{\mathbf{U}}^{(n-1)}$ and $\mathbf{V}^{(n-1)}$, solve the convex quadratic approximation of (8) to obtain $\tilde{\mathbf{A}}^{(n)}$
Step 4	Compute step size $\gamma^{(n)} = \gamma^{(n-1)}(1 - a\gamma^{(n-1)})$
Step 5	Update $\mathbf{A}^{(n)}$ using $\mathbf{A}^{(n)} = \tilde{\mathbf{A}}^{(n)} + \gamma^{(n)}(\mathbf{A}^{(n-1)} - \tilde{\mathbf{A}}^{(n)})$
Step 6	Test for convergence and if the test fails return to Step 1

4. NUMERICAL EXPERIMENTS

We now apply both measures of ED and RD to examine their effects on the signal optimization formulation as well as their effects on delay and Doppler-shift estimation.

4.1. Signal Synthesis

Our consideration focuses on a MIMO radar with 2 co-located linear arrays of transmission and reception antennas, each having 4 sensors. Each transmission waveform is a linear combination of $k = 1, \cdots, 16$ orthonormal basis signals $s_k(t) = \cos\left((2k-1)\omega_0 t\right), \omega_0 = 2\pi \times 5\ \text{rad}/\mu\text{s}$, each of duration $T = 1\mu s$. Since the peak of the AF f_{mm} is constrained to have the value of $P_0 = 1$ at $(0, 0)$, we can stipulate all sidelobe amplitude to be lower than $0.2P_0$ and test the following two cases of designing different widths of the main lobe

Case 1: We stipulate the main lobe height at $(\pm.03\mu\text{s}, 0)$ and at $(0, \pm 2\pi \times .1\text{rad}/\mu\text{s})$ to be $0.4P_0$

Case 2: We stipulate the main lobe height at $(\pm.02\mu\text{s}, 0)$ and at $(0, \pm 2\pi \times .05\text{rad}/\mu\text{s})$ to be $0.4P_0$.

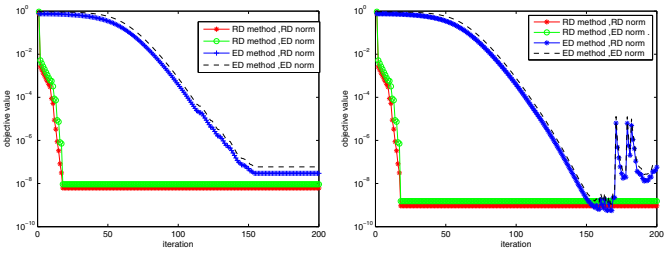

(a) Case 1 (b) Case 2

Fig. 1. Convergence of design algorithm in iterations

Fig. 1 (a) and (b) show the convergence rates of the designs in Case 1 and Case 2 respectively. The black and blue lines show the convergence of the ED objective function measured in ED and RD respectively, whereas the green and red lines shows the convergence of the RD objective function measured respectively in ED and RD. It can be observed that in both cases 1 and 2, the ED design takes almost 10 times the number of iterations to converge than the RD design. The slower convergence of the ED design can be explained partly by examining the approximate objective functions of Eqs. (9) and (13). We can see that $(\mathbf{U}^{(n-1)}\mathbf{\Sigma}^{(n-1)}\mathbf{V}^{(n-1)^H})$ in $\hat{d}_{\text{E}}$ is a general matrix that is not necessarily unitary, whereas $\tilde{\mathbf{U}}^{(n-1)}\mathbf{V}^{(n-1)^H}$ in $\hat{d}_{\text{R}_2}$ is always unitary. Since it is desired to minimize the difference between the design covariance matrix and $\mathbf{I}$, then the matrix $\tilde{\mathbf{A}}^{(n)}$ in $\hat{d}_{\text{R}_2}$ should be close to unitary. Hence in the search of $\tilde{\mathbf{A}}^{(n)}$ under RD, the search space will be constrained to a relevant space smaller than a more general space in the case of searching under ED. As a result, we would expect the design of the covariance matrix under RD to converge faster than that under ED.

For Case 1, both ED and RD objective functions converge to a low value, yielding synthesized signals that satisfy the requirements. As the constraint becomes tighter as in Case 2, when the required width of the main lobe of the AF becomes narrower, it is observed that the objective function using ED does not converge properly anymore, i.e., the final value is no longer stable. However, in this case, the use of RD still converges well showing greater robustness.

4.2. The Ambiguity Functions

In the optimization process, we put a mask on the amplitude of the AF $f_{mm}(\tau,\nu), m = 1,\cdots,M$ so that they satisfy certain requirements. Case 1 and Case 2 differ in the specification of the width of the mainlobe – being narrower in Case 2. Fig 2 shows the sections of the MIMO AF (Eq. (5)) along the time-delay and the Doppler shift axes for the optimized ED and RD designs. Here, it can be observed that both ED and RD designs satisfy the mask.

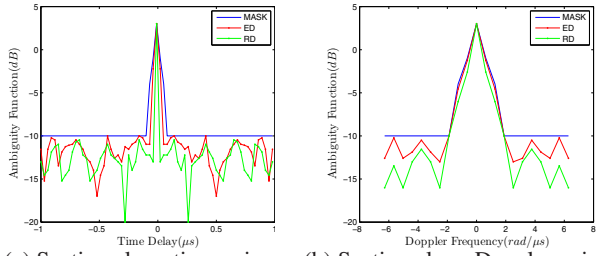

(a) Section along time axis (b) Section along Doppler axis

Fig. 2. Case 1: Mask and MIMO AF sections

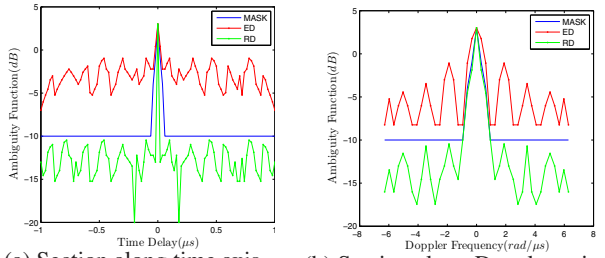

(a) Section along time axis (b) Section along Doppler axis

Fig. 3. Case 2: Mask and MIMO AF sections

Fig 3 shows Case 2 in which the width of the mainlobe of the AF is substantially narrower in both the time-delay and the Doppler shift axes. We use the optimized signals obtained by the ED and the RD designs. It is observed that while the RD design still well satisfies the mask requirements, the ED design fails by a significant margin. This is due to the poor convergence behaviour of the algorithm in the ED case.

4.3. Distance and Velocity Estimation Error

Here, we set the scenario of having N targets at distances $d_1,\cdots,d_N$ from the reference point of the arrays, travelling with velocities $v_1,\cdots,v_N$, respectively, all arriving at an angle θ to the normal of the transmission antenna. The receiver signal-to-noise ratio (SNR) is assumed to be 3dB. For the ambiguity function of the returned signal, any local maximum of correlation between received signals and time-frequency shifted transmitted signal that is greater than the threshold, is considered a target candidate. The threshold is determined by the Neyman-Pearson criterion fixing the false alarm rate at 0.08. For an SNR of 3dB, this stipulates [17] the maximum sidelobe/mainlobe ratio to be $\epsilon \approx 0.2$. We now carry out the estimation of the distances and velocities of targets using the MIMO AF of Eq. (5) generated by the different optimally designed signals. For each set of transmitted signals estimating the distances and velocities of the N targets, we respectively define the average normalized square errors of distance and velocity estimation as:

$$\bar{e}_{\mathrm{d}}^2 = \frac{1}{N}\left[\sum_{n=1}^{N}\left(e_{\mathrm{d}_n}/d_n\right)^2\right]; \qquad \bar{e}_{\mathrm{v}}^2 = \frac{1}{N}\left[\left(e_{\mathrm{v}_n}/v_n\right)^2\right]$$

Table 2 shows the sum of the normalized squared errors $(\bar{e}_{\mathrm{d}}^2 + \bar{e}_{\mathrm{v}}^2)$ in the estimation of the distances and velocities of two targets using the signal AF in design Case 1. Recall that in Case 1, the objective function of both ED and RD designs converges. However, it can be observed here that using the RD design still yields higher accuracies in the estimation than using the ED design. The superior accuracies of the RD design are especially significant when the targets are close together in the last two columns.

Table 2. $(\bar{e}_{\mathrm{d}}^2 + \bar{e}_{\mathrm{v}}^2)$ for Case 1

Locations (km) & velocities (km/h)	(30, 800) (30.5, 800)	(30, 800) (30.1, 800)	(30.1, 800) (30.05, 800)	(30.05, 800) (30.02, 800)
ED	3.46e-7	8.76e-7	7.86e-4	6.74e-2
RD	3.36e-7	5.56e-7	6.35e-6	5.53e-4

Table 3. $(\bar{e}_{\mathrm{d}}^2 + \bar{e}_{\mathrm{v}}^2)$ for Case 2

Locations (km) & velocities (km/h)	(30, 800) (30.5, 800)	(30, 800) (30.1, 800)	(30.1, 800) (30.05, 800)	(30.05, 800) (30.02, 800)
ED	2.46e-7	4.57e-4	5.36e-3	7.34e-2
RD	4.36e-8	6.56e-8	5.35e-7	6.36e-5

Table 3 shows the total squared error in the estimation of the distances and velocities of two targets using the signal AF in design Case 2. Here, since the objective function of the ED design did not converge properly, we expect that the estimations carried out using the ED design are much inferior to those using the RD design. Indeed, we can observe that the accuracies of the estimations using the RD design are substantially higher. We can also observe that the estimations using the RD design in Case 2 is higher in accuracy than the corresponding estimations using the RD design in Case 1. This is because the AF in Case 2 has a narrower mainlobe thus the mutual interference of the two target mainlobes is reduced.

5. CONCLUSION

We seek for a design of the MIMO radar transmission signal by minimizing the distance between the covariance matrix of the signal vector and the identity matrix, while suppressing the AF sidelobes in time and Doppler frequency shift. We argue that since covariance matrices are not freely structured but are Hermitian and positive semi-definite, the true distance should be formulated in RD. Simplifying the optimizations in the Euclidean and Riemannian spaces, we notice that the RD algorithm only needs to search for the optimum in a smaller space close to unitary, resulting in faster convergence of the optimization using RD. The RD signal design also proves to have higher accuracy in both the location and velocity estimation of the targets. As well, it yields signals which are more robust to tight constraints (such as narrower mainlobe) on the AF.

6. REFERENCES

[1] J. Li and P. Stoica (ed.), *MIMO Radar Signal Processing*, John Wiley & Sons, Inc., Hoboken, N.J., 2009.

[2] I. Oppermann and B. S. Vucetic, "Complex spreading sequences with a wide range of correlation properties", *IEEE Trans. on Comm.*, vol. 45, no. 3, pp. 365-375, Mar., 1997.

[3] P. Stoica, J. Li, and Y. Xie, "On probing signal design for MIMO radar", *IEEE Trans. on Sig. Proc.*, vol. 55, no. 8, pp. 4151-4161, Aug., 2007.

[4] Y. Wang, X. Wang, H. Liu, and Z.-Q. Luo, "On the design of constant modulus probing signals for MIMO radar", *IEEE Tran. on Sig. Proc.*, vol. 60, no. 8, pp. 4432-4438, Aug., 2012.

[5] J. Li, P. Stoica, X. Zheng, "Signal synthesis and receiver design for MIMO radar imaging", *IEEE Trans. on Sig. Proc.*, vol. 56, no. 8, pp. 3959-3968, Aug., 2008.

[6] H. He, P. Stoica, and J. Li, "Designing unimodular sequence sets with good correlations – including an application to MIMO radar", *IEEE Trans. on Sig. Proc.*, vol. 57, no. 11, pp. 4391-4405, Nov., 2009.

[7] G. H. Golub and C. F. Van Loan, *Matrix Computations*, Johns Hopkins University Press, 3rd ed., 1996.

[8] Y. Li and K. M. Wong, "Riemannian distances for signal classification by power spectral density", *IEEE J. of Selected Topics in Sig. Proc*., vol. 7, no.4, pp. 655-669, Aug., 2013.

[9] G. San Antonio, D. R. Fuhrmann and F. C. Robey, "MIMO radar ambiguity functions," in *IEEE J. of Selected Topics in Sig. Proc.*, vol. 1, no. 1, pp. 167-p177, June 2007.

[10] C.-Y. Chen and P. P. Vaidyanathan, "MIMO radar ambiguity properties and optimization using frequency-hopping waveforms", *IEEE Trans. on Sig. Proc.*, vol. 56, no. 12, pp. 5926-5936, Dec., 2008.

[11] H. L. Van Trees, *Detection, Estimation, and Modulation Theory*, Pt. III, Wiley, 1971.

[12] R. Sharma, "Analysis of MIMO radar ambiguity functions and implications on clear region," *2010 IEEE Radar Conf.*, Washington, DC, 2010.

[13] W. Khan, I. M. Qureshi and K. Sultan, "Ambiguity function of phased MIMO radar with colocated antennas and its properties," in *IEEE Geosc. and Rem. Sens. Lett.*, vol. 11, no. 7, pp. 1220-1224, July 2014.

[14] M. Razaviyayn, M. Hong and Z.-Q. Luo, "A unified convergence analysis of block successive minimization methods for nonsmooth optimization" *SIAM J. Opt.*, vol. 23, no. 2, pp. 1126–1153, 2013.

[15] G. Scutari, F. Facchinei, and L. Lampariello, "Parallel and distributed methods for constrained nonconvex optimization — Part I: Theory." *IEEE Trans. Signal Process.*, vol. 65, no. 8, pp. 1929–1944, 2017.

[16] M. Hong, M. Razaviyayn, Z. Luo and J. Pang, "A unified algorithmic framework for block-structured optimization involving big data: With applications in machine learning and signal processing," in *IEEE Sig. Proc. Magazine*, vol. 33, no. 1, pp. 57-77, Jan. 2016.

[17] K. M. Wong, Z.-Q. Luo and Q. Jin, "Design of optimum signals for simultaneous estimation of time delay and Doppler shift", *IEEE Trans. on Sig. Proc.*, vol. 41, no. 6, pp. 2141–2154, June, 1993.